Matter and Radiation at Extremes

RESEARCH ARTICLE

pubs.aip.org/aip/mre

Featured

High-pressure minerals and new lunar mineral changesite-(Y) in Chang'e-5 regolith

Cite as: Matter Radiat. Extremes 9, 027401 (2024); doi: 10.1063/5.0148784
Submitted: 2 March 2023 • Accepted: 9 November 2023 •
Published Online: 6 February 2024

Jing Yang[1] **and Wei Du**[2,3,a)]

AFFILIATIONS

[1] Center for Lunar and Planetary Sciences, Institute of Geochemistry, Chinese Academy of Sciences, Guiyang 550081, China
[2] State Key Laboratory of Ore Deposit Geochemistry, Institute of Geochemistry, Chinese Academy of Sciences (CAS), Guiyang 550081, China
[3] CAS Center for Excellence in Comparative Planetology, Hefei 230026, China

Note: Paper published as part of the Special Topic on High Pressure Science 2024
[a)] **Author to whom correspondence should be addressed:** duwei@mail.gyig.ac.cn

ABSTRACT

Forty-five years after the Apollo and Luna missions, China's Chang'e-5 (CE-5) mission collected ~1.73 kg of new lunar materials from one of the youngest basalt units on the Moon. The CE-5 lunar samples provide opportunities to address some key scientific questions related to the Moon, including the discovery of high-pressure silica polymorphs (seifertite and stishovite) and a new lunar mineral, changesite-(Y). Seifertite was found to be coexist with stishovite in a silica fragment from CE-5 lunar regolith. This is the first confirmed seifertite in returned lunar samples. Seifertite has two space group symmetries (*Pnc*2 and *Pbcn*) and formed from an α-cristobalite-like phase during "cold" compression during a shock event. The aftershock heating process changes some seifertite to stishovite. Thus, this silica fragment records different stages of an impact process, and the peak shock pressure is estimated to be ~11 to 40 GPa, which is much lower than the pressure condition for coexistence of seifertite and stishovite on the phase diagram. Changesite-(Y), with ideal formula $(Ca_8Y)\square Fe^{2+}(PO_4)_7$ (where □ denotes a vacancy) is the first new lunar mineral to be discovered in CE-5 regolith samples. This newly identified phosphate mineral is in the form of columnar crystals and was found in CE-5 basalt fragments. It contains high concentrations of Y and rare earth elements (REE), reaching up to ~14 wt. % $(Y,REE)_2O_3$. The occurrence of changesite-(Y) marks the late-stage fractional crystallization processes of CE-5 basalts combined with silicate liquid immiscibility. These new findings demonstrate the significance of studies on high-pressure minerals in lunar materials and the special nature of lunar magmatic evolution.

I. HIGH-PRESSURE MINERALS

Collision is one of the most important dynamic processes shaping the evolution of bodies in the Solar System.[1] The transient pressure and temperature rise during high-velocity collisions usually cause shock metamorphism of target rocks, such as deformation, phase transformation, decomposition, melting, and vaporization,[2,3] and thus phase transformation plus specific shock-deformation features such as planar deformation are widely used to constrain the transient temperature and pressure conditions as well as the magnitude of impact events.[4,5] The surface of the Moon is dominated by densely distributed craters at various scales, indicating a complex impact history. High-pressure minerals are expected to form during these massive impact events and can provide essential information about the cratering processes on the Moon. In the past decade, many high-pressure minerals (e.g., coesite, stishovite, seifertite, ringwoodite, wadsleyite, reidite, tissintite, and donwilhelmsite) have been observed in lunar meteorites.[6–12] However, high-pressure minerals in Apollo and Luna returned samples have rarely been reported. Only stishovite and a single x-ray diffraction (XRD) peak of a silica grain that was assigned to d110 reflection of seifertite were reported in an Apollo regolith breccia 15299, but no further and conclusive evidence confirmed the existence of seifertite.[13]

Silica (SiO_2) is one of the primary components of terrestrial planets, and thus its high-pressure polymorphs provide important information for understanding the structure and physical properties of Earth's interior and natural dynamic events (e.g., impacts) on planetary surfaces.[14–16] Coesite, stishovite, and seifertite have

previously been found in Martian meteorites (e.g., Shergotty, Zagami, Northwest Africa 856, and Northwest Africa 8657),[14–18] lunar meteorites (Asuka-881757 and Northwest Africa 4734),[6,7] and Apollo regolith breccia 15299.[13] The coesite in Martian meteorite 8657 is found in silica glass and/or nano-phase maskelynite distributed within shock-induced melt regions. These coesite grains appear in a silica–maskelynite assemblage (type I), or as needle grains (type II), or as granular grains embedded in maskelynite (type III).[18] Hu *et al.*[18] proposed that the coesite in the silica–maskelynite assemblage was formed through crystallization from SiO_2-rich melt along the maskelynite–silica interface in mesostasis, and that the other two types may have been inverted from stishovite during the decompression process. Similar to the type III coesite in Martian meteorites, the coesite in the lunar meteorite Asuka-881757 also presents as small granular inclusions within amorphous silica grains found in shock-melt pockets and has been proposed to have formed through back-transformation during decompression.[6]

Stishovite in Martian meteorites displays different occurrences and has been proposed to have formed through a variety of mechanisms: (1) Intergrowths of fine-grained stishovite and zagamiite [a new high-pressure hexaluminosilicate phase with general formula $(Ca,Na)(Al,Fe,Mg)_2(Si,Al,\square)_4O_{11}$, where $\square$ represents a vacancy] or coexistence of needle-shaped stishovites with a variety of dense minerals, including zagamiite, a new type of tissintite [tissintite-II, $(Ca,Mg,Na,\square_{0.14})(Al,Fe,Mg)Si_2O_6$], liebermannite, and Ca,Na-aluminosilicate with hollandite-type structure (lingunite–stöfflerite) occurring in shock-melt pockets and veins.[16,17,19–24] These assemblages are considered to have been crystallized from a feldspathic melt at shock pressures of ~20 GPa or lower.[21,22,25] (2) Individual stishovite grains in shock-melt pockets that might have formed through a solid-state transformation from tridymite or cristobalite.[16,25] (3) In Tissint, a shergottite Martian meteorite, stishovite either is associated with olivine (1–2 μm microcrystalline stishovite + olivine) inside a melt pocket or occurs as tiny needles coexisting with ringwoodite and clinopyroxene within the matrix of a thin shock-melt vein.[26,27] The metastable assemblage (stishovite + clinopyroxene + ringwoodite) is proposed to have crystallized via rapid quenching during decompression.[27] (4) Stishovite identified in amorphous silica that occurs as irregular grains among maskelynite, pigeonite, and Ti–magnetite in NWA 2975.[28]

In contrast to Martian meteorites, stishovite in lunar meteorites has an angular shape (size ~100 nm) enclosed in amorphous silica grains in shock-melt pockets, or occurs as thin platelets coexisting with cristobalite in silica grains with lamellae-like texture far from the shock-melt veins, or has acicular morphology accompanied by seifertite, cristobalite, and silica glass in silica grains with tweed-like texture in or adjacent to shock-melt veins.[6,7] The crystallographic orientation of stishovite is correlated with the twinned cristobalite, indicating that they were transformed from cristobalite during an impact event.[7] Moreover, needle-like or lamellar-like stishovite was found in a shock-melt vein in Apollo regolith breccia 15299, which is the first report of high-pressure polymorphs from returned lunar samples.[13] The stishovite occurs along the fractures of the silica grain, which also contains quartz, tridymite, and silica glass. Kaneko *et al.*[13] suggested that the silica grain in 15299 might have been melted once along the fractures and recrystallized to form stishovite at pressures above 8 GPa during the Imbrium impact or subsequent local impact event(s) in the Procellarum KREEP Terrane of the Moon.

Seifertite is an α-PbO_2-type silica, named after Friedrich Seifert by El Goresy *et al.*[17] The seifertite-bearing silica grains in both Martian and lunar meteorites show a tweed-like texture.[7,14,16,25] These seifertite crystals generally occur within a (sub)orthogonal framework of amorphous lamellae and have been proposed to be transformed from cristobalite or tridymite.[7,14–17,25] On the other hand, high-pressure experiments and theoretical calculations suggest that seifertite is stable above ~85 GPa,[29,30] and seifertite and stishovite coexist stably at ~50 to 90 GPa and ~500 to 2500 K.[31] High-pressure diamond anvil cell (DAC) experiments revealed that the suggested starting materials tridymite and cristobalite transform directly to seifertite at pressures >40 GPa.[31,32] Considering its heat sensitivity and the high post-shock temperatures, seifertite cannot survive heavy impact events (>42 GPa).[3] Therefore, the presence of seifertite in Martian and lunar meteorites is difficult to explain. Kubo *et al.*[33] conducted *in situ* x-ray diffraction (XRD) measurements under high-pressure–temperature conditions and revealed that seifertite could have metastably formed from cristobalite at pressures down to ~11 GPa. These experimental results provide very important information to help solve the puzzle of how seifertite can occur in meteorite samples or returned lunar samples that have experienced impact events.

Chang'e-5 (CE-5 hereinafter), China's first lunar sample return mission, which landed at 43.06°N, 51.92°W in the Northern Oceanus Procellarum,[34] has successfully returned 1.731 kg of lunar samples.[35,36] Fragments in CE-5 regolith samples are predominantly composed of low- to medium-Ti basalt clasts with a young crystallization age of ~2.0 Ga,[37–39] and some other fragments include agglutinate, glass (round glass beads and irregularly shaped glass fragments), and breccias (fragmental breccia and crystalline breccia).[36,40–42] Recently, the shock-produced high-pressure phases seifertite and stishovite have been found in a single, discrete silica fragment from a CE-5 lunar regolith sample CE5C0800YJFM00101GP (hereinafter 01GP) (Fig. 1).[43]

The silica fragment containing seifertite and stishovite in CE-5 sample 01GP exhibits a tweed-like texture (Figs. 1 and 2), similar to silica grains containing seifertite in Martian and lunar meteorites. In addition to seifertite and stishovite, amorphous silica and α-cristobalite-like phases are also present. The silica fragment contains two types of sets of crystallographically oriented amorphous silica lamellae (Fig. 2). One features a suborthogonal pattern consisting of two sets of lamellae along a major plane (~100 to 500 nm thick) and a minor plane (~10 to 50 nm thick), respectively. The other is characterized as a subhexagonal pattern consisting of three sets of lamellae (widths ~100 to 200 nm).[43] Pang *et al.*[43] conducted a detailed analysis of the microtexture of the silica fragment in the CE-5 regolith and found that seifertite crystallites occur within the suborthogonal framework and orientate parallel to the micro-twins' boundaries of the α-cristobalite-like phase, whereas stishovite crystallites are bound by three sets of amorphous lamellae, not compatible with the tetragonal twinning texture of α-cristobalite-like phase (Fig. 2). They further proposed that the seifertite is a metastable phase between α-cristobalite and stishovite, that seifertite could form from α-cristobalite during the compression process,[31,44] that some of the seifertite transformed to stishovite during the subsequent temperature increase,[33] and that the α-cristobalite-like phase may

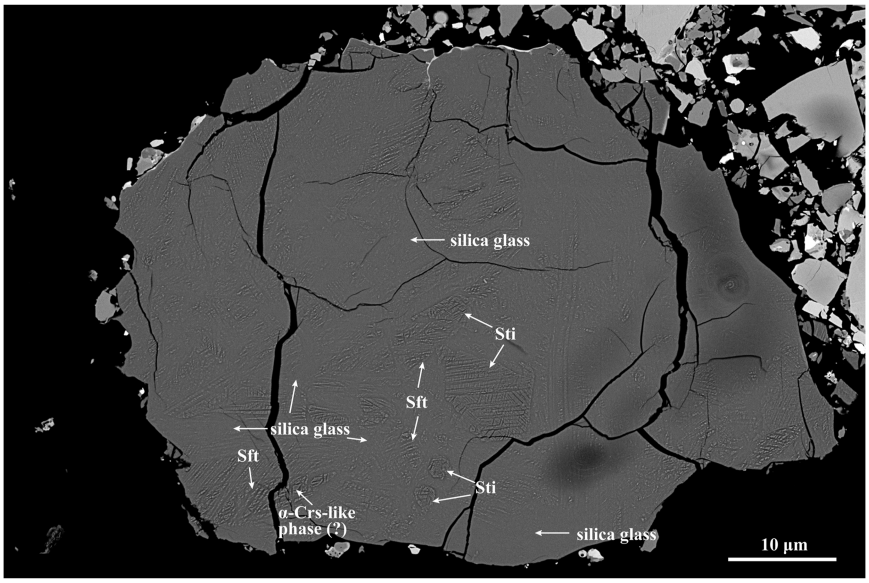

FIG. 1. Backscattered electron (BSE) image of the seifertite- and stishovite-bearing silica fragment in CE-5 regolith sample 01GP. The phase in the smooth area around the seifertite, stishovite, and α-cristobalite-like phases is amorphous silica. Sft, seifertite; Sti, stishovite; α-Crs-like, α-cristobalite-like. Reproduced with permission from Pang *et al.*, "New occurrence of seifertite and stishovite in Chang'E-5 regolith," Geophys. Res. Lett. **49**(12), e2022GL098722 (2022). Copyright 2022 John Wiley & Sons.

be an as-yet unidentified intermediate phase like the cristobalite-II and cristobalite X-I that form during the phase transition sequence from α-cristobalite to seifertite.[44] Thus, the silica fragment records different stages of a shock event. This new discovery of the coexistence of an α-cristobalite-like phase, seifertite, and stishovite in the CE-5 lunar regolith is consistent with the results of *in situ* experiments on the kinetic behavior of silica polymorphs, which showed that seifertite can be formed at ~11 GPa and 1100 K through an α-cristobalite-like phase (cristobalite-XI).[33] Pang *et al.*[43] therefore suggested that the seifertite and stishovite were formed as the result of an impact with peak pressure between ~11 and 40 GPa. Taking account of a crater size calculation (giving a lower limit on diameter of ~3 to 32 km) and analysis of remote sensing data,[45–47] they proposed that the Aristarchus crater could be the source of the silica fragment containing high-pressure polymorphs found in CE-5 regolith sample 01GP.

II. NEW MINERAL CHANGESITE-(Y)

Petrological and geochemical features of CE-5 basalts, such as their enrichment in FeO and incompatible elements and the KREEP-like rare earth element (REE) patterns that they exhibit, indicate that they were formed through extensive fractional crystallization.[41,42,48,49] The CE-5 basalt fragments show igneous

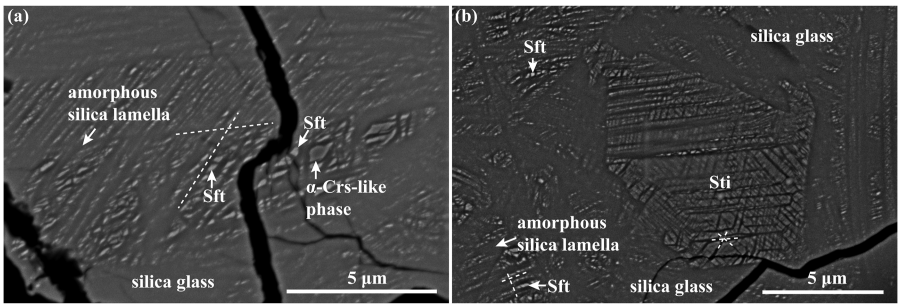

FIG. 2. BSE images showing the tweed-like texture of the silica fragment in Fig. 1. The white dashed lines represent the orientations of the amorphous silica lamellae. Sft, seifertite; Sti, stishovite; α-Crs-like, α-cristobalite-like. Reproduced with permission from Pang *et al.*, "New occurrence of seifertite and stishovite in Chang'E-5 regolith," Geophys. Res. Lett. **49**(12), e2022GL098722 (2022). Copyright 2022 John Wiley & Sons.

textures and consist mainly of clinopyroxene, plagioclase, olivine, and ilmenite, with minor amounts of K-feldspar, silica, Ca-phosphates (apatite and merrillite), and Zr-rich minerals such as baddeleyite and zirconolite.[37,48,50] The modal mineralogy of phosphate is up to 1.4 wt. %.[36,37,48] The high content of phosphorus and REE in CE-5 basalts raises the possibility of crystallization of phosphate with incompatible elements enriched.

Changesite-(Y) was found in CE-5 basalts by a research group at the Beijing Research Institute of Uranium Geology (BRIUG), and the identification of this new mineral was approved by the Commission on New Minerals, Nomenclature and Classification (CNMNC) of the International Mineralogical Association (IMA) in 2022 (IMA No. 2022-023).[51] Changesite-(Y) belongs to the cerite supergroup. The grains show columnar morphology, with a crystal length of ~2 to 30 μm. XRD results showed that changesite-(Y) has trigonal symmetry with space group $R3c$ with cell parameters a = 10.3957(4) Å and c = 37.207(2) Å.[51] Changesite-(Y) could be the sixth new lunar mineral known so far.

Changesite-(Y), which has the ideal formula $(Ca_8Y)\square Fe^{2+}(PO_4)_7$,[51] falls into the merrillite group of phosphates of lunar occurrence. Previous studies have shown that lunar merrillite, $(Mg,Fe^{2+},Mn^{2+})_2[Ca_{18-x}(Y,REE)_x](Na_{2-x})(P,Si)_{14}O_{56}$, contains high concentrations of Y+REE, reaching up to ~18 wt. % as $(Y,REE)_2O_3$, or over 3 Y+REE atoms per 56 O atoms.[52–54] We have also identified some Y+REE-rich phosphate crystals in basalt fragments from the CE-5 sample 01GP, and their chemical compositions are almost the same as that of changesite-(Y). These grains typically contain ~1.0 to 2.3 Y+REE atoms per 56 O atoms (Table I). As shown in Fig. 3(a), the slope of the regression line between the sum of Y+REE and Ca is −1.17, approaching −1.2, indicating that the substitution is simply $(Y+REE)_{2,Ca\ site} + \square_{Na\ site} \leftrightarrow Ca_3$, where the vacancy □ is presumably at the Na site.[54] In addition, the number of Na atoms goes to zero at 2 Y+REE (Table I), which is consistent with the vacancy occurring primarily at the Na site and not at other, Ca, sites.

To determine how charges are balanced through the substitutions mentioned above, we plot the number of Y+REE cations vs several of the notable compositional variables, including the number of Na and Si cations, in Fig. 3(b). It can be seen that the number of Na cations decreases as the sum Y+REE increases, confirming that charges for REE substitution between 0 and 2 Y+REE cations per 56 O atoms are balanced primarily by a vacancy on the Na site. Furthermore, for between 0 and 2 Y+REE per 56 O, ~5% of the substitution is $(Y+REE)^{3+}_{Ca\ site} + Si^{4+}_{T} \leftrightarrow Ca^{2+}_{Ca\ site} + P^{5+}_{T}$, which is confirmed by the correlation of Si and Y+REE [Fig. 3(b)]. For more than 2 Y+REE per 56 O, the substitution should be balanced mainly by increasing Si substitution for P, because the Na site is fully vacated at 2 Y+REE cations per 56 O atoms. In addition, the number of divalent cations (Fe + Mn + Mg) in changesite-(Y) found in 01GP is more than 2 (Table I) and varies with Y+REE, although with much scatter [Fig. 3(b)], which indicates some mixing of these elements on the Ca sites and possibly on the Na site as well.

Phosphates are typically found within intercumulus melt pockets (mesostasis), representing the final stages of basaltic crystallization.[55–57] As mentioned above, CE-5 basalts formed through a large degree of fractional crystallization and have a high content of incompatible elements. During the crystallization of CE-5 basalts, these incompatible elements will be further enriched in the residual liquid. According to thermodynamic modeling results, the liquid line of descent of CE-5 basalts intersects the two-silicate liquid field after ~75% fractional crystallization.[50,58] High-field-strength cations such as P, Y, and REE preferentially go into the Fe-rich liquid during the silicate liquid immiscibility (SLI) mechanism,[59–63] and so merrillite tends to crystallize from the immiscible Fe-rich liquids. Scanning electron microscope (SEM) examination of CE-5 basalt fragments revealed that changesite-(Y) occurs in mesostasis regions and coexists with fayalite, clinopyroxene, plagioclase, ilmenite, apatite, baddeleyite, cristobalite, troilite, and Si–K-rich glass (Fig. 4). These mesostasis regions are characterized by "globules" of a Si–K-rich glass set within a fayalite matrix, which are commonly referred to as "sieve" textures and are characteristic of conjugate immiscible liquids (such as in the SLI mechanism).[55–57,64–66] Therefore, fractional crystallization plus the

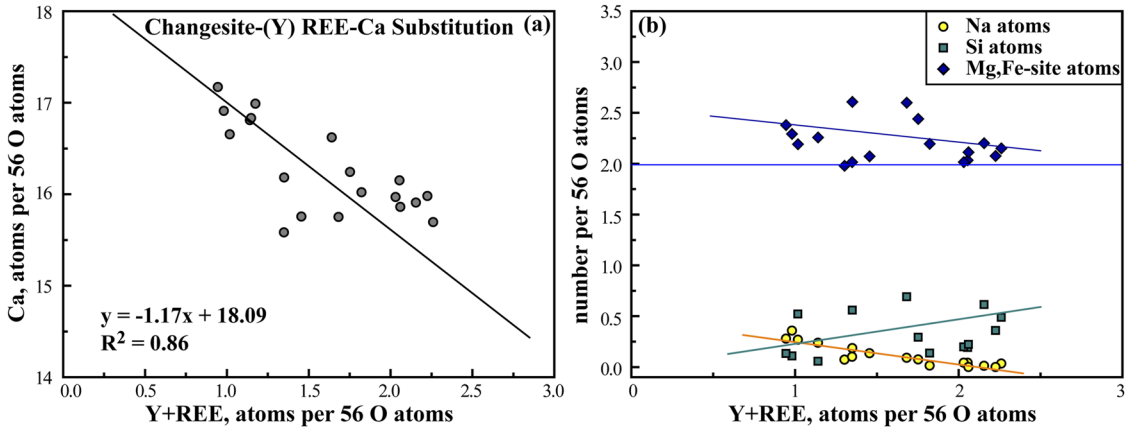

FIG. 3. Y+REE vs other cations in changesite-(Y), expressed as cations per 56 O atoms. Data are listed in Table I. (a) Y+REE vs Ca; the regression equation is for the line shown, fitted to the changesite-(Y) grains in CE-5 sample 01GP. (b) Y+REE vs Na, Si, and Mg,Fe-site atoms in changesite-(Y). Mg,Fe-site atoms include Mg, Fe, and Mn.

TABLE I. Changesite-(Y) compositions in CE-5 regolith sample 01GP.[a]

	No. 1	No. 2	No. 3	No. 4	No. 5	No. 6	No. 7	No. 8	No. 9	No. 10	No. 11	No. 12	No. 13	No. 14	No. 15	No. 16	No. 17
P_2O_5	42.85	42.74	42.43	40.17	39.08	38.9	41.7	40.6	41.1	42.5	40.7	40.2	39.7	41.0	41.2	41.2	40.0
SiO_2	0.14	0.28	1.36	4.02	7.61	6.27	0.35	1.76	0.75	0.34	1.42	1.23	1.55	0.48	0.50	0.56	0.90
TiO_2	0.02	0.05	0.03	n.a.	n.a.	n.a.	n.a.	n.a.	0.04	0.06	0.05	0.02	0.06	b.d.	0.02	0.03	0.04
Al_2O_3	0.07	0.08	0.20	n.a.	n.a.	n.a.	n.a.	n.a.	0.08	0.04	0.47	b.d.	0.07	b.d.	b.d.	b.d.	0.02
FeO	6.32	6.46	6.23	6.10	6.04	6.03	6.59	7.77	6.77	6.77	7.25	6.33	6.49	6.06	6.03	6.23	6.13
MnO	0.11	0.09	0.06	0.06	0.05	0.07	0.07	0.11	0.04	0.06	0.05	0.06	0.06	0.05	0.05	0.06	0.06
MgO	0.33	0.33	0.32	0.15	0.10	0.11	b.d.	0.03	0.35	0.30	0.35	0.06	0.05	0.02	b.d.	0.05	b.d.
CaO	40.76	41.02	40.76	38.09	37.28	38.0	37.9	37.5	38.6	41.6	38.4	36.9	37.4	38.1	37.7	37.4	37.3
BaO	0.03	0.04	b.d.	n.a.	n.a.	n.a.	n.a.	n.a.	0.03	b.d.	b.d.	b.d.	b.d.	0.02	b.d.	b.d.	0.03
Na_2O	0.32	0.48	0.36	0.18	0.10	0.14	0.02	0.12	0.10	0.37	0.24	0.04	0.02	0.06	0.06	b.d.	b.d.
K_2O	0.15	0.18	0.28	n.a.	n.a.	n.a.	n.a.	n.a.	0.02	0.04	0.03	0.04	0.09	0.04	0.06	0.04	0.05
Y_2O_3	1.68	1.45	1.59	2.21	2.00	2.19	2.76	2.62	2.74	1.45	2.02	2.96	2.76	2.45	2.41	2.12	2.44
La_2O_3	0.89	0.74	0.76	1.18	1.09	1.09	1.42	1.27	1.27	0.69	0.97	1.98	2.00	1.80	1.80	2.26	2.19
Ce_2O_3	2.14	1.92	1.89	2.86	2.66	2.59	3.46	3.28	2.98	1.75	2.47	4.41	4.42	4.30	4.18	4.77	4.79
Pr_2O_3	0.280	0.189	0.239	0.341	0.286	0.244	0.424	0.310	0.343	0.258	0.302	0.577	0.634	0.581	0.557	0.499	0.550
Nd_2O_3	1.308	1.066	1.257	1.682	1.582	1.502	2.052	1.925	1.985	1.124	1.591	2.508	2.282	2.420	2.438	2.386	2.384
Sm_2O_3	0.301	0.274	0.272	n.a.	n.a.	n.a.	n.a.	n.a.	0.489	0.315	0.374	0.578	0.585	0.563	0.594	0.540	0.553
Gd_2O_3	0.459	0.500	0.373	0.636	0.585	0.623	0.828	0.766	0.783	0.287	0.516	0.791	0.660	0.737	0.731	0.507	0.779
Dy_2O_3	0.420	0.295	0.301	0.536	0.445	0.558	0.632	0.535	0.547	0.271	0.350	0.659	0.444	0.413	0.428	0.346	0.647
Total	98.6	98.2	98.7	98.2	98.9	98.3	98.2	98.6	99.2	98.3	97.8	99.4	99.4	99.0	98.8	99.0	98.9
$(Y+REE)_2O_3$	7.47	6.43	6.68	9.45	8.65	8.79	11.57	10.71	11.14	6.14	8.59	14.46	13.79	13.27	13.14	13.43	14.32
P	13.96	13.92	13.70	13.13	12.49	12.61	13.91	13.48	13.68	13.86	13.57	13.50	13.33	13.73	13.81	13.80	13.55
Si	0.055	0.108	0.520	1.553	2.873	2.399	0.137	0.690	0.293	0.132	0.560	0.488	0.614	0.191	0.197	0.222	0.360
Sum (P,Si)	14.02	14.03	14.22	14.68	15.36	15.01	14.05	14.17	13.97	14.00	14.13	13.98	13.95	13.92	14.01	14.02	13.91
Ti	0.005	0.014	0.007	0.000	0.000	0.000	0.000	0.000	0.013	0.018	0.015	0.007	0.017	0.000	0.005	0.008	0.011
Al	0.029	0.034	0.088	0.000	0.000	0.000	0.000	0.000	0.039	0.020	0.216	0.006	0.032	0.003	0.005	0.007	0.009
Fe	2.035	2.077	1.986	1.969	1.908	1.931	2.171	2.549	2.225	2.184	2.389	2.100	2.150	2.005	1.996	2.062	2.048
Mn	0.035	0.028	0.020	0.019	0.017	0.023	0.023	0.036	0.013	0.021	0.015	0.018	0.020	0.016	0.018	0.020	0.020
Mg	0.187	0.188	0.184	0.084	0.055	0.062	0.000	0.017	0.203	0.174	0.205	0.033	0.031	0.014	0.000	0.032	0.008
Ca	16.81	16.91	16.65	15.76	15.07	15.58	16.02	15.75	16.24	17.17	16.18	15.69	15.91	16.15	15.97	15.86	15.98
Ba	0.004	0.005	0.000	0.000	0.000	0.000	0.000	0.000	0.004	0.000	0.000	0.000	0.000	0.003	0.000	0.000	0.004
Na	0.238	0.357	0.268	0.135	0.072	0.100	0.014	0.090	0.073	0.279	0.186	0.034	0.012	0.042	0.042	0.000	0.000
K	0.075	0.087	0.135	0.000	0.000	0.000	0.000	0.000	0.012	0.022	0.017	0.021	0.045	0.022	0.030	0.018	0.026
Y+REE	1.14	0.98	1.02	1.45	1.30	1.35	1.82	1.68	1.75	0.95	1.35	2.26	2.15	2.06	2.03	2.06	2.22
Sum of cations	20.56	20.68	20.36	19.42	18.43	19.05	20.05	20.12	20.58	20.83	20.57	20.17	20.37	20.31	20.10	20.07	20.33

[a]n.a., not analyzed; b.d., below the detection limit.

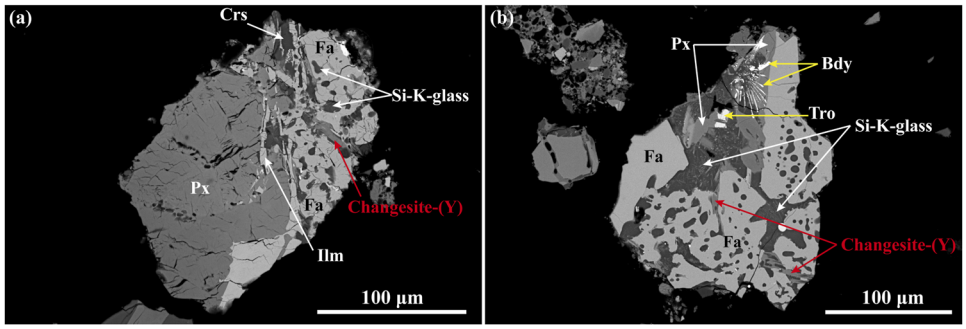

FIG. 4. BSE images of changesite-(Y) in basalt fragments from CE-5 regolith sample 01GP. Fa, fayalite; Px, pyroxene; Pl, plagioclase; Crs, cristobalite; Bdy, baddeleyite; Tro, troilite.

SLI mechanism leads to the liquids from which changesite-(Y) crystallizes as well as to changesite-(Y) having very high concentrations of Y and REE.

III. PROSPECTS

The size of the crater responsible for the formation of stishovite and seifertite discovered in CE-5 regolith can be estimated using shock wave physics models.[67] The shock peak pressure in this case is estimated to be 11–40 GPa, as discussed by Pang *et al.*,[43] and the shock duration is estimated to be 0.1–1.0 s on the basis of the time–temperature transformation curves of stishovite and seifertite.[33] If the impact angle is vertical, a crater with diameter of 3–32 km can then be generated, and in view of the impact angle and the pressure gradient in the crater, this range provides a lower limit on the diameter of the crater from which the stishovite and seifertite originated.[43] On the basis of remote sensing observations, the exotic ejecta in regolith distributed in the CE-5 landing region come predominantly from five proximal and four distant craters.[46,47] The four distant craters, namely, Mairan G (diameter ~6 km), Aristarchus (~40 km), Harpalus (~40 km), and Copernicus (~94 km) fall within the estimated crater size range. Considering that both seifertite and stishovite are easily disturbed by thermal heating, Aristarchus (formation age ~280 Ma[68]), which is the youngest among the four distant craters and has silica-rich materials exposed in its interior, rim, and ejecta,[69–71] is the most likely candidate for the source of the host rock of seifertite and stishovite. Therefore, the discovery of seifertite and stishovite in the CE-5 sample confirms the remote sensing observations and provides evidence for the existence of impact ejecta from distant craters in CE-5 regolith samples. This demonstrates the potential for finding diverse lithologies with different crystallization ages outside the CE-5 sampling site.

As noted in Sec. I, the presence of seifertite in shocked meteorites has previously been considered puzzling, given the shock conditions generated by impact events on planetary surfaces. The "new" discovery of seifertite in CE-5 lunar regolith confirms *in situ* high-pressure and high-temperature experimental results on this silica polymorph, which revealed that seifertite can be present as a metastable phase at pressures as low as ~11 GPa, owing to the clear difference in kinetics between metastable seifertite and stable stishovite formations.[33] Although the shocked silica fragment found in CE-5 regolith is small ($50 \times 60\ \mu m^2$, Fig. 1), the coexistence of seifertite, stishovite, amorphous silica, and α-cristobalite-like phases, as well as their formation mechanisms, make this silica fragment a natural sample for examining the kinetic behavior of high-pressure silica polymorphs. Furthermore, the significant differences in formation conditions (pressure–temperature–time) of high-pressure silica polymorphs between equilibrium static and dynamic high-pressure experiments demonstrate that we must be cautious in using phase diagrams to constrain the shock conditions recorded by high-pressure minerals in meteorites and terrestrial impact craters.[72,73] More work needs to be conducted to reveal the kinetics of various high-pressure polymorphs during dynamic impact processes. Therefore, the discovery of high-pressure silica polymorphs in only 30 mg of CE-5 regolith highlights the potential of multiplying high-pressure minerals in lunar materials, which could provide new information about impact processes on the Moon and other planetary bodies in the early Solar System.

Changesite-(Y), the sixth new lunar mineral to be discovered, has extremely high contents of Y and REE. It crystallized from the residual melts of Fe-rich CE-5 basalts that had experienced fractional crystallization and the SLI mechanism. The formation of changesite-(Y) implies that other new minerals with very high Fe, P, Y, or REE content might also have formed during the late-stage crystallization of CE-5 basalts. On the other hand, new minerals discovered in lunar returned samples and lunar meteorites can also reflect their formation conditions, providing key information about the magmatic activity, thermal evolution, and impact history of the Moon.

IV. ANALYTICAL METHODS

The sample was examined using an FEI Scios Dual-Beam focused ion beam/scanning electron microscope (FIB-SEM) equipped with an energy dispersive spectrometer (EDS) at the Center for Lunar and Planetary Sciences (CLPS), Institute of Geochemistry, Chinese Academy of Sciences (IGCAS), Guiyang. The operating voltage and beam current were 20 kV and 1.6 nA, respectively.

Quantitative analyses of phosphates were conducted with an electron probe micro-analyzer (EPMA; JEOL JXA-8530FPlus) at the State Key Laboratory of Ore Deposit Geochemistry (SKLODG), IGCAS. Measurements were performed with an accelerating voltage of 15 kV and a beam current of 10 nA. Elements measured using the $K\alpha$ lines were counted on peak for 20 s (Si, Ti, Al, Cr, Fe, Mn, and Mg) and 10 s (Na, K, F, and Cl); elements measured using the $L\alpha$ lines were counted on peak for 30 s (Y, La, Ce, Pr, Nd, Sm, Gd, Dy, and Ba). The standards for elements in phosphates were pyrope for Si, Al, Cr, Fe, Mn, and Mg, rutile for Ti, apatite for Ca, P, and F, plagioclase for Na, orthoclase for K, barite for Ba, tugtupite for Cl, and Buenópolis monazite [$(Ce,La)PO_4$] for La, Ce, Pr, Nd, Sm, Gd, Tb, Dy, and Y.

ACKNOWLEDGMENTS

We thank the China National Space Administration (CNSA) for providing the CE-5 sample CE5C0800YJFM00101GP. We would like to thank Yuanyun Wen and Xiang Li for their assistance with SEM observations and EPMA analyses, respectively. This work was supported by the B-Type Strategic Priority Research Program of the Chinese Academy of Sciences (Grant No. XDB 41000000), the National Natural Science Foundation of China (Grant Nos. 41773052, 41973058, and 42003054), the Key Research Program of the Chinese Academy of Sciences (Grant No. ZDBS-SSW-JSC007-10), the Pre-Research Project on Civil Aerospace Technologies funded by the CNSA (Grant No. D020201), and the China Postdoctoral Science Foundation (Grant No. 2020M680155).

AUTHOR DECLARATIONS

Conflict of Interest

The authors have no conflicts to disclose.

Author Contributions

Jing Yang: Conceptualization (equal); Formal analysis (lead); Writing – original draft (lead); Writing – review & editing (equal).

Wei Du: Conceptualization (lead); Funding acquisition (equal); Writing – original draft (equal); Writing – review & editing (equal).

DATA AVAILABILITY

The data that support this study are available from the corresponding authors upon reasonable request.

REFERENCES

[1]H. Hiesinger and J. W. Head III, "New views of lunar geoscience: An introduction and overview," Rev. Mineral. Geochem. **60**(1), 1 (2006).

[2]F. Langenhorst and A. Deutsch, "Shock metamorphism of minerals," Elements **8**(1), 31 (2012).

[3]D. Stöffler, C. Hamann, and K. Metzler, "Shock metamorphism of planetary silicate rocks and sediments: Proposal for an updated classification system," Meteorit. Planet. Sci. **53**(1), 5 (2018).

[4]P. Gillet and A. E. Goresy, "Shock events in the solar system: The message from minerals in terrestrial planets and asteroids," Annu. Rev. Earth Planet. Sci. **41**(1), 257 (2013).

[5]N. Tomioka and M. Miyahara, "High-pressure minerals in shocked meteorites," Meteorit. Planet. Sci. **52**(9), 2017 (2017).

[6]E. Ohtani, S. Ozawa, M. Miyahara, Y. Ito, T. Mikouchi, M. Kimura, T. Arai, K. Sato, and K. Hiraga, "Coesite and stishovite in a shocked lunar meteorite, Asuka-881757, and impact events in lunar surface," Proc. Natl. Acad. Sci. U. S. A. **108**(2), 463 (2011).

[7]M. Miyahara, S. Kaneko, E. Ohtani, T. Sakai, T. Nagase, M. Kayama, H. Nishido, and N. Hirao, "Discovery of seifertite in a shocked lunar meteorite," Nat. Commun. **4**(1), 1737 (2013).

[8]J. Fritz, A. Greshake, M. Klementova, R. Wirth, L. Palatinus, R. G. Trønnes, V. A. Fernandes, U. Böttger, and L. Ferrière, "Donwilhelmsite, [$CaAl_4Si_2O_{11}$], a new lunar high-pressure Ca-Al-silicate with relevance for subducted terrestrial sediments," Am. Mineral. **105**(11), 1704 (2020).

[9]W. Xing, Y. Lin, C. Zhang, M. Zhang, S. Hu, B. A. Hofmann, T. Sekine, L. Xiao, and L. Gu, "Discovery of reidite in the lunar meteorite Sayh al Uhaymir 169," Geophys. Res. Lett. **47**(21), e2020GL089583, https://doi.org/10.1029/2020gl089583 (2020).

[10]A.-C. Zhang, Q.-T. Jiang, N. Tomioka, Y.-J. Guo, J.-N. Chen, Y. Li, N. Sakamoto, and H. Yurimoto, "Widespread tissintite in strongly shock-lithified lunar regolith breccias," Geophys. Res. Lett. **48**(5), e2020GL091554, https://doi.org/10.1029/2020gl091554 (2021).

[11]A.-C. Zhang, W.-B. Hsu, C. Floss, X.-H. Li, Q.-L. Li, Y. Liu, and L. A. Taylor, "Petrogenesis of lunar meteorite Northwest Africa 2977: Constraints from in situ microprobe results," Meteorit. Planet. Sci. **45**(12), 1929 (2010).

[12]J. A. Barrat, M. Chaussidon, M. Bohn, P. Gillet, C. Göpel, and M. Lesourd, "Lithium behavior during cooling of a dry basalt: An ion-microprobe study of the lunar meteorite Northwest Africa 479 (NWA 479)," Geochim. Cosmochim. Acta **69**(23), 5597 (2005).

[13]S. Kaneko, M. Miyahara, E. Ohtani, T. Arai, N. Hirao, and K. Sato, "Discovery of stishovite in Apollo 15299 sample," Am. Mineral. **100**(5-6), 1308 (2015).

[14]T. G. Sharp, A. E. Goresy, B. Wopenka, and M. Chen, "A post-stishovite SiO_2 polymorph in the meteorite Shergotty: Implications for impact events," Science **284**(5419), 1511 (1999).

[15]A. E. Goresy, L. Dubrovinsky, T. G. Sharp, S. K. Saxena, and M. Chen, "A monoclinic post-stishovite polymorph of silica in the Shergotty meteorite," Science **288**(5471), 1632 (2000).

[16]A. El Goresy, L. Dubrovinsky, T. G. Sharp, and M. Chen, "Stishovite and post-stishovite polymorphs of silica in the Shergotty meteorite: Their nature, petrographic settings versus theoretical predictions and relevance to Earth's mantle," J. Phys. Chem. Solids **65**(8–9), 1597 (2004).

[17]A. El Goresy, P. Dera, T. G. Sharp, C. T. Prewitt, M. Chen, L. Dubrovinsky, B. Wopenka, N. Z. Boctor, and R. J. Hemley, "Seifertite, a dense orthorhombic polymorph of silica from the Martian meteorites Shergotty and Zagami," Eur. J. Mineral. **20**(4), 523 (2008).

[18]S. Hu, Y. Li, L. Gu, X. Tang, T. Zhang, A. Yamaguchi, Y. Lin, and H. Changela, "Discovery of coesite from the martian shergottite Northwest Africa 8657," Geochim. Cosmochim. Acta **286**, 404 (2020).

[19]M. Miyahara, N. Tomioka, and L. Bindi, "Natural and experimental high-pressure, shock-produced terrestrial and extraterrestrial materials," Prog. Earth Planet. Sci. **8**(1), 59 (2021).

[20]C. Ma, O. Tschauner, and J. R. Beckett, "A new high pressure calcium aluminosilicate ($CaAl_2Si_{3.5}O_{11}$) in Martian meteorites: Another after-life for plagioclase and connections to the CAS phase," in The 48th Lunar and Planetary Science Conference, Abstract #1128, 2017.

[21]C. Ma, O. Tschauner, and J. R. Beckett, "A closer look at Martian meteorites: Discovery of the new mineral zagamiite, $CaAl_2Si_{3.5}O_{11}$, a shock-metamorphic, high-pressure, calcium aluminosilicate," in The 9th International Conference on Mars, Abstract #6138, 2019.

[22]C. Ma, O. Tschauner, J. R. Beckett, G. R. Rossman, C. Prescher, V. B. Prakapenka, H. A. Bechtel, and A. MacDowell, "Liebermannite, $KAlSi_3O_8$, a new shock-metamorphic, high-pressure mineral from the Zagami Martian meteorite," Meteorit. Planet. Sci. **53**(1), 50 (2018).

[23]O. Tschauner, C. Ma, J. G. Spray, E. Greenberg, and V. Prakapenka, "Stöfflerite, (Ca,Na)(Si,Al)4O8 in the hollandite structure: A new high-pressure polymorph of anorthite from martian meteorite NWA 856," Am. Mineral. **106**(4), 650 (2021).

[24]P. Beck, P. Gillet, L. Gautron, I. Daniel, and A. El Goresy, "A new natural high-pressure (Na,Ca)-hexaluminosilicate [$(Ca_xNa_{1-x})Al_{3+x}Si_{3-x}O_{11}$] in shocked Martian meteorites," Earth Planet. Sci. Lett. **219**(1-2), 1 (2004).

[25]A. El Goresy, P. Gillet, M. Miyahara, E. Ohtani, S. Ozawa, P. Beck, and G. Montagnac, "Shock-induced deformation of Shergottites: Shock-pressures and perturbations of magmatic ages on Mars," Geochim. Cosmochim. Acta **101**, 233 (2013).

[26]I. P. Baziotis, Y. Liu, P. S. DeCarli, H. Jay Melosh, H. Y. McSween, R. J. Bodnar, and L. A. Taylor, "The Tissint Martian meteorite as evidence for the largest impact excavation," Nat. Commun. **4**, 1404 (2013).

[27]E. L. Walton, T. G. Sharp, J. Hu, and J. Filiberto, "Heterogeneous mineral assemblages in martian meteorite Tissint as a result of a recent small impact event on Mars," Geochim. Cosmochim. Acta **140**, 334 (2014).

[28]Q. He, L. Xiao, J. B. Balta, I. P. Baziotis, W. Hsu, and Y. Guan, "Petrography and geochemistry of the enriched basaltic shergottite Northwest Africa 2975," Meteorit. Planet. Sci. **50**(12), 2024 (2015).

[29]D. M. Teter, R. J. Hemley, G. Kresse, and J. Hafner, "High pressure polymorphism in silica," Phys. Rev. Lett. **80**(10), 2145 (1998).

[30]L. S. Dubrovinsky, S. K. Saxena, P. Lazor, R. Ahuja, O. Eriksson, J. M. Wills, and B. Johansson, "Experimental and theoretical identification of a new high-pressure phase of silica," Nature **388**(6640), 362 (1997).

[31]L. S. Dubrovinsky, N. A. Dubrovinskaia, S. K. Saxena, F. Tutti, S. Rekhi, T. Le Bihan, G. Shen, and J. Hu, "Pressure-induced transformations of cristobalite," Chem. Phys. Lett. **333**(3–4), 264 (2001).

[32]N. A. Dubrovinskaia, L. S. Dubrovinsky, S. K. Saxena, F. Tutti, S. Rekhi, and T. Le Bihan, "Direct transition from cristobalite to post-stishovite α-PbO_2-like silica phase," Eur. J. Mineral. **13**(3), 479 (2001).

[33]T. Kubo, T. Kato, Y. Higo, and K.-i. Funakoshi, "Curious kinetic behavior in silica polymorphs solves seifertite puzzle in shocked meteorite," Sci. Adv. **1**(4), e1500075 (2015).

[34]J. Wang, Y. Zhang, K. Di, M. Chen, J. Duan, J. Kong, J. Xie, Z. Liu, W. Wan, Z. Rong, B. Liu, M. Peng, and Y. Wang, "Localization of the Chang'e-5 lander using radio-tracking and image-based methods," Remote Sens. **13**(4), 590 (2021).

[35]W. Yang and Y. Lin, "New lunar samples returned by Chang'e-5: Opportunities for new discoveries and international collaboration," Innovation **2**(1), 100070 (2021).

[36]C. Li, H. Hu, M.-F. Yang, Z.-Y. Pei, Q. Zhou, X. Ren, B. Liu, D. Liu, X. Zeng, G. Zhang, H. Zhang, J. Liu, Q. Wang, X. Deng, C. Xiao, Y. Yao, D. Xue, W. Zuo, Y. Su, W. Wen, and Z. Ouyang, "Characteristics of the lunar samples returned by the Chang'E-5 mission," Natl. Sci. Rev. **9**(2), nwab188 (2022).

[37]X. Che, A. Nemchin, D. Liu, T. Long, C. Wang, M. D. Norman, K. H. Joy, R. Tartese, J. Head, B. Jolliff, J. F. Snape, C. R. Neal, M. J. Whitehouse, C. Crow, G. Benedix, F. Jourdan, Z. Yang, C. Yang, J. Liu, S. Xie, Z. Bao, R. Fan, D. Li, Z. Li, and S. G. Webb, "Age and composition of young basalts on the Moon, measured from samples returned by Chang'e-5," Science **374**(6569), 887 (2021).

[38]Q.-L. Li, Q. Zhou, Y. Liu, Z. Xiao, Y. Lin, J.-H. Li, H.-X. Ma, G.-Q. Tang, S. Guo, X. Tang, J.-Y. Yuan, J. Li, F.-Y. Wu, Z. Ouyang, C. Li, and X.-H. Li, "Two-billion-year-old volcanism on the Moon from Chang'e-5 basalts," Nature **600**, 54 (2021).
[39]S. Boschi, X.-L. Wang, H. Hui, Z. Yin, Y. Guan, H. Hu, W. Zhang, J. Chen, and W. Li, "Compositional variability of 2.0-Ga lunar basalts at the Chang'e-5 landing site," J. Geophys. Res.: Planets **128**(5), e2022JE007627, https://doi.org/10.1029/2022je007627 (2023).
[40]T. Long, Y. Qian, M. D. Norman, K. Miljkovic, C. Crow, J. W. Head, X. Che, R. Tartèse, N. Zellner, X. Yu, S. Xie, M. Whitehouse, K. H. Joy, C. R. Neal, J. F. Snape, G. Zhou, S. Liu, C. Yang, Z. Yang, C. Wang, L. Xiao, D. Liu, and A. Nemchin, "Constraining the formation and transport of lunar impact glasses using the ages and chemical compositions of Chang'e-5 glass beads," Sci. Adv. **8**(39), eabq2542 (2022).
[41]W. Yang, Y. Chen, H. Wang, H.-C. Tian, H. Hui, Z. Xiao, S.-T. Wu, D. Zhang, Q. Zhou, H.-X. Ma, C. Zhang, S. Hu, Q.-L. Li, Y. Lin, X.-H. Li, and F.-Y. Wu, "Geochemistry of impact glasses in the Chang'e-5 regolith: Constraints on impact melting and the petrogenesis of local basalt," Geochim. Cosmochim. Acta **335**, 183 (2022).
[42]K. Zong, Z. Wang, J. Li, Q. He, Y. Li, H. Becker, W. Zhang, Z. Hu, T. He, K. Cao, Z. She, X. Wu, L. Xiao, and Y. Liu, "Bulk compositions of the Chang'E-5 lunar soil: Insights into chemical homogeneity, exotic addition, and origin of landing site basalts," Geochim. Cosmochim. Acta **335**, 284 (2022).
[43]R. Pang, J. Yang, W. Du, A. Zhang, S. Liu, and R. Li, "New occurrence of seifertite and stishovite in Chang'E-5 regolith," Geophys. Res. Lett. **49**(12), e2022GL098722, https://doi.org/10.1029/2022gl098722 (2022).
[44]A. Černok, K. Marquardt, R. Caracas, E. Bykova, G. Habler, H.-P. Liermann, M. Hanfland, M. Mezouar, E. Bobocioiu, and L. S. Dubrovinsky, "Compressional pathways of α-cristobalite, structure of cristobalite X-I, and towards the understanding of seifertite formation," Nat. Commun. **8**(1), 15647 (2017).
[45]Y. Qian, L. Xiao, J. W. Head, C. H. van der Bogert, H. Hiesinger, and L. Wilson, "Young lunar mare basalts in the Chang'e-5 sample return region, northern Oceanus Procellarum," Earth Planet. Sci. Lett. **555**, 116702 (2021).
[46]Y. Qian, L. Xiao, J. W. Head, C. Wöhler, R. Bugiolacchi, T. Wilhelm, S. Althoff, B. Ye, Q. He, Y. Yuan, and S. Zhao, "Copernican-aged (<200 Ma) impact ejecta at the Chang'e-5 landing site: Statistical evidence from crater morphology, morphometry, and degradation models," Geophys. Res. Lett. **48**(20), e2021GL095341, https://doi.org/10.1029/2021gl095341 (2021).
[47]Y. Qian, L. Xiao, Q. Wang, J. W. Head, R. Yang, Y. Kang, C. H. van der Bogert, H. Hiesinger, X. Lai, G. Wang, Y. Pang, N. Zhang, Y. Yuan, Q. He, J. Huang, J. Zhao, J. Wang, and S. Zhao, "China's Chang'e-5 landing site: Geology, stratigraphy, and provenance of materials," Earth Planet. Sci. Lett. **561**, 116855 (2021).
[48]H.-C. Tian, H. Wang, Y. Chen, W. Yang, Q. Zhou, C. Zhang, H.-L. Lin, C. Huang, S.-T. Wu, L.-H. Jia, L. Xu, D. Zhang, X.-G. Li, R. Chang, Y.-H. Yang, L.-W. Xie, D.-P. Zhang, G.-L. Zhang, S.-H. Yang, and F.-Y. Wu, "Non-KREEP origin for Chang'e-5 basalts in the Procellarum KREEP Terrane," Nature **600**, 59 (2021).
[49]H.-C. Tian, W. Yang, D. Zhang, H. Zhang, L. Jia, S. Wu, Y. Lin, X. Li, and F. Wu, "Petrogenesis of Chang'E-5 mare basalts: Clues from the trace elements in plagioclase," Am. Mineral. **108**(9), 1669 (2023).
[50]Q. He, Y. Li, I. Baziotis, Y. Qian, L. Xiao, Z. Wang, W. Zhang, B. Luo, C. R. Neal, J. M. D. Day, F. Pan, Z. She, X. Wu, Z. Hu, K. Zong, and L. Wang, "Detailed petrogenesis of the unsampled Oceanus Procellarum: The case of the Chang'e-5 mare basalts," Icarus **383**, 115082 (2022).
[51]R. Miyawaki, F. Hatert, M. Pasero, and S. J. Mills, "IMA Commission on New Minerals, Nomenclature and Classification (CNMNC) – Newsletter 69," Eur. J. Mineral. **34**, 463 (2022).
[52]B. L. Jolliff, L. A. Haskin, R. O. Colson, and M. Wadhwa, "Partitioning in REE-saturating minerals: Theory, experiment, and modelling of whitlockite, apatite, and evolution of lunar residual magmas," Geochim. Cosmochim. Acta **57**(16), 4069 (1993).
[53]J. M. Hughes, B. L. Jolliff, and M. E. Gunter, "The atomic arrangement of merrillite from the Fra Mauro Formation, Apollo 14 lunar mission: The first structure of merrillite from the Moon," Am. Mineral. **91**(10), 1547 (2006).
[54]B. L. Jolliff, J. M. Hughes, J. J. Freeman, and R. A. Zeigler, "Crystal chemistry of lunar merrillite and comparison to other meteoritic and planetary suites of whitlockite and merrillite," Am. Mineral. **91**(10), 1583 (2006).
[55]J. F. Pernet-Fisher, G. H. Howarth, Y. Liu, Y. Chen, and L. A. Taylor, "Estimating the lunar mantle water budget from phosphates: Complications associated with silicate-liquid-immiscibility," Geochim. Cosmochim. Acta **144**, 326 (2014).
[56]A. M. Álvarez-Valero, J. F. Pernet-Fisher, and L. M. Kriegsman, "Petrologic history of lunar phosphates accounts for the water content of the Moon's mare basalts," Geosciences **9**(10), 421 (2019).
[57]N. J. Potts, R. Tartèse, M. Anand, W. van Westrenen, A. A. Griffiths, T. J. Barrett, and I. A. Franchi, "Characterization of mesostasis regions in lunar basalts: Understanding late-stage melt evolution and its influence on apatite formation," Meteorit. Planet. Sci. **51**(9), 1555 (2016).
[58]J. Yang, D. Ju, R. Pang, R. Li, J. Liu, and W. Du, "Significance of silicate liquid immiscibility for the origin of young highly evolved lithic clasts in Chang'E-5 regolith," Geochim. Cosmochim. Acta **340**, 189 (2023).
[59]C. R. Neal and L. A. Taylor, "Lunar granite petrogenesis and the process of silicate liquid immiscibility: The barium problem," in *Workshop on Moon in Transition: Apollo 14 KREEP, and Evolved Lunar Rocks*, edited by G. J. Taylor and P. H. Warren (LPI Contribution, 1989), p. 89.
[60]C. R. Neal and L. A. Taylor, "The nature of barium partitioning between immiscible melts: A comparison of experimental and natural systems with reference to lunar granite petrogenesis," in *Proceedings of the 19th Lunar and Planetary Science Conference* (LPI Contribution, 1989), p. 209.
[61]C. K. Shearer, J. J. Papike, and M. N. Spilde, "Trace-element partitioning between immiscible lunar melts: An example from naturally occurring lunar melt inclusions," Am. Mineral. **86**(3), 238 (2001).
[62]I. V. Veksler and B. Charlier, in *Silicate Liquid Immiscibility in Layered Intrusions*, *Layered Intrusions*, edited by B. Charlier, O. Namur, R. Latypov, and C. Tegner (Springer Netherlands, Dordrecht, 2015), p. 229.
[63]A. L. Gullikson, J. J. Hagerty, M. R. Reid, J. F. Rapp, and D. S. Draper, "Silicic lunar volcanism: Testing the crustal melting model," Am. Mineral. **101**(10), 2312 (2016).
[64]M. J. Rutherford, P. C. Hess, and G. H. Daniel, "Experimental liquid line of descent and liquid immiscibility for basalt 70017," in *Proceedings of the 5th Lunar Science Conference* (LPI Contribution, 1974), Vol. 1, p. 569.
[65]P. C. Hess, M. J. Rutherford, R. N. Guillemette, F. J. Ryerson, and H. A. Tuchfeld, "Residual products of fractional crystallization of lunar magmas: An experimental study," in *Proceedings of the Sixth Lunar Science Conference* (LPI Contribution, 1975), p. 895.
[66]B. Charlier and T. L. Grove, "Experiments on liquid immiscibility along tholeiitic liquid lines of descent," Contrib. Mineral. Petrol. **164**(1), 27 (2012).
[67]H. J. Melosh, *Impact Cratering: A Geologic Process* (Oxford University Press, 1989).
[68]M. Zanetti, A. Stadermann, B. Jolliff, H. Hiesinger, C. H. van der Bogert, and J. Plescia, "Evidence for self-secondary cratering of Copernican-age continuous ejecta deposits on the Moon," Icarus **298**, 64 (2017).
[69]T. D. Glotch, P. G. Lucey, J. L. Bandfield, B. T. Greenhagen, I. R. Thomas, R. C. Elphic, N. Bowles, M. B. Wyatt, C. C. Allen, K. D. Hanna, and D. A. Paige, "Highly silicic compositions on the Moon," Science **329**(5998), 1510 (2010).
[70]R. N. Clegg-Watkins, B. L. Jolliff, M. J. Watkins, E. Coman, T. A. Giguere, J. D. Stopar, and S. J. Lawrence, "Nonmare volcanism on the Moon: Photometric evidence for the presence of evolved silicic materials," Icarus **285**, 169 (2017).
[71]T. D. Glotch, E. R. Jawin, B. T. Greenhagen, J. T. Cahill, D. J. Lawrence, R. N. Watkins, D. P. Moriarty, N. Kumari, S. Li, P. G. Lucey *et al.*, "The scientific value of a sustained exploration program at the Aristarchus plateau," Planet. Sci. J. **2**, 136 (2021).
[72]J. Hu and T. G. Sharp, "Formation, preservation and extinction of high-pressure minerals in meteorites: Temperature effects in shock metamorphism and shock classification," Prog. Earth Planet. Sci. **9**(1), 6 (2022).
[73]O. Tschauner and C. Ma, "Discovering high-pressure and high-temperature minerals," in *Celebrating the International Year of Mineralogy: Progress and Landmark Discoveries of the Last Decades*, edited by L. Bindi and G. Cruciani (Springer Nature Switzerland, Cham, 2023), p. 169.